Downloaded 09/27/18 to 50.203.133.34. Redistribution subject to SEG license or copyright; see Terms of Use at http://library.seg.org/

# Far offset P-to-S "elastic impedance" for lithology and partial gas saturation (fizz water) identification: Applications with well logs.

*Ezequiel F. Gonzalez*, Tapan Mukerji, Gary Mavko, and Reinaldo J. Michelena.*
*Stanford Rock Physics Laboratory.*

**Summary**

In this paper, we present a formulation of P-to-S "elastic impedance" (PSEI), assuming the validity of convolutional model for PS converted waves and weak contrast between layers. We show how, for a particular analytically defined angle, PSEI can theoretically give a *direct density estimator*. Two applications with real well logs are shown: PSEI as best lithology differentiator in an Orinoco Belt example (also applicable to reservoirs with small acoustic impedance contrast between sands and shales), and PSEI to discriminate between commercial gas saturations and fizz water using Eastern Venezuela logs.

**Introduction**

Seismic lithology identification, and distinguishing between fizz water and commercial gas saturations are two specific problems that in many cases cannot be solved with only P-wave seismic information. The phenomenon of sand-shale crossover with depth can give rise to significant overlap in acoustic impedance, making it difficult to discriminate sands and shales from P-wave data alone. Attempting to seismically differentiate homogeneously mixed fizz water with low gas saturation from higher gas saturations is difficult. The abrupt reduction in Vp with the first few percent of gas controls the seismic response. Therefore, usually only the presence of gas but not the saturation can be detected with PP seismic.

Use of P-to-S converted waves (PS) has been suggested as a source of additional information that can help in these two situations, for example, Engelmark (2000) in the case of imaging reservoirs with low-impedance contrast, and Wu (2000), and Zhu et al (2000) for distinguishing high vs. low gas saturation. However, those works propose using PP and/or PS reflectivity (Rpp, Rps), which are interface properties. Landro (1999) derived "shear wave elastic impedance" (SEI), assuming weak contrast and small incidence angle using a linear approximation of Rps.

In this paper, we present a formulation of PS "elastic impedance" (PSEI) not limited to small incidence angles, which at one defined angle (theoretically) gives a direct estimation of density. We also analyze why, when ρ is the key elastic property, PSEI can be the best discriminator of reservoir conditions. Additionally, we present two practical applications of PSEI using well log information. First, we show how PSEI better discriminates lithology in sequences with small Ip contrast. Orinoco well logs were used in this example. Second, we show, using Eastern Venezuela well logs, how through PSEI it is possible to distinguish fizz water from commercial gas concentrations.

**Theory**

Assuming the validity of convolutional model for PS converted waves and weak contrast between layers, "PS elastic impedance" (PSEI) can be defined as:

$$PSEI(\theta p) = \rho^{c} Vs^{d} \qquad (eq.1)$$

Where, θp is P-wave incidence angle (approximately), and *c* and *d* are given by:

$$c = \frac{K \sin\theta p}{\sqrt{\frac{1}{K^2} - \sin^2\theta p}} \left( 2\sin^2\theta p - \frac{1}{K^2} - 2\cos\theta p \sqrt{\frac{1}{K^2} - \sin^2\theta p} \right) \qquad (eq.2)$$

$$d = \frac{4K \sin\theta p}{\sqrt{\frac{1}{K^2} - \sin^2\theta p}} \left( \sin^2\theta p - \cos\theta p \sqrt{\frac{1}{K^2} - \sin^2\theta p} \right) \qquad (eq.3)$$

Where, constant K is the average Vs/Vp. The derivation is in the same spirit as the derivations of far offset elastic impedance (e.g. Connolly, 1999). Equations 2 and 3 are non-linear trigonometric equations in θp. The root, $\theta_{pd}$=arctan(1/K), of the equation *d*=0 defines a specific angle at which the exponent *c* equals –1. Hence at this specific angle PSEI($\theta_{pd}$) = 1/ρ. We choose positive offsets of CCP gathers to obtain these expressions.

Figure 1 displays the behavior of c and d exponents as a function of incidence angle (K=0.4). It can be seen how for $\theta_{pd}$, *c*=-1, and *d*=0. At near offsets (small angles) Vs and ρ terms contribute equally to PSEI. On the other hand, for mid-to-large offsets the ρ term dominates PSEI behavior. The asymmetric contribution or "decoupling" between Vs and ρ role on PSEI can be exploited in discriminating different reservoir properties. This decoupling was also noticed by Wu (2000), studying Rps for a particular AVO case. Here, we derive the theoretical underpinning and generality of the decoupling effect, and show how an average of Vs/Vp determines the angle at which the effect is maximized. Although, as shown above, theoretically is possible to get a direct value of density from PSEI at a single angle, clearly in practice it will be very difficult. Small variations of angle estimation raise important differences between true and PSEI estimated densities. Added to this are problems due to the approximate

Downloaded 09/27/18 to 50.203.133.34. Redistribution subject to SEG license or copyright; see Terms of Use at http://library.seg.org/



knowledge of K, noise in seismic data, possible processing artifacts, and imperfections of PS seismic inversion to obtain PSEI. However, this fact only limits the possibility of getting absolute density values. It does not preclude the potential use of PSEI to discriminate between reservoir situations where density is the key elastic property. In other words, though it will be difficult to directly *estimate* absolute densities through PSEI, it will still be possible to *classify* based on relative density variations.

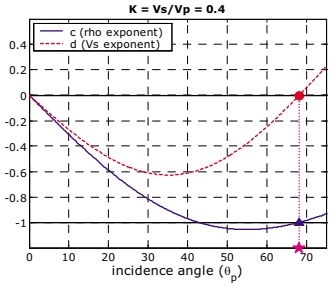


Figure 1: PSEI exponents *c* and *d* as a function of incidence angle (Vs/Vp=0.4). The star indicates the angle where PSEI=1/ρ.

**Lithology Identification: Orinoco Belt example**

The Orinoco Belt is located in the southern part of the Eastern Basin of Venezuela, north of the Orinoco River, covering an area of approximately 700 km$^2$. The major productive units are fluvial-deltaic sands of early to middle Miocene. Complex sand-body architectures with discontinuities caused by low-permeability facies are characteristic in the area. Heavy oil production in the Orinoco Belt is mainly carried out with horizontal wells; therefore, it is very important to precisely locate sands units as best as possible before drilling.

In order to investigate which seismic attribute better discriminates (elastically) lithology in the area, the statistical rock physics methodology presented by Mukerji et al (2001) was applied, using a set of logs from a reference well. Figure 2 shows some of the available logs, after editing for bad caliper and data inconsistencies. Colored dots indicate each of the 3 a priori defined lithology groups, viz. sands, shales, and lignites. These groups were identified based on cutoff levels of gamma ray (gr<50 for sands; gr>80 for shales) and density logs (ρ < 1.9 gr/cc for lignites). Figure 3 presents histograms of Vp, Vs, ρ, and Ip calculated for each lithology group from log data. Although, Vp, Vs, and ρ distributions of sands and shales show certain separation, the overlap in Ip is remarkable. This is not a peculiarity of the studied area alone; in fact, it is a common situation in relatively shallow clastic reservoirs. At shallow depths, sands usually have smaller Ip than shales. With increasing depth, there is a crossover and Ip for sands become greater than that for shales. Consequently, for some range of depths there is small or no Ip contrast between sands and shales.

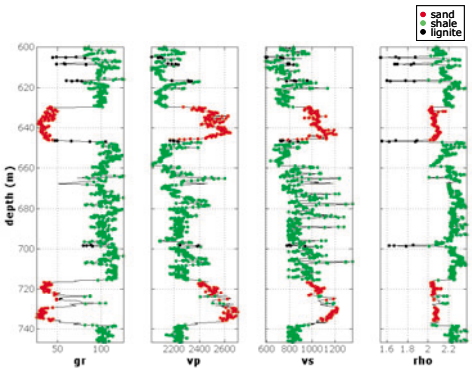


Figure 2: Log data of the reference well (after editing). Colors indicate the assigned lithology based on gamma ray (gr) thresholds for sands and shales, and density threshold for lignites.

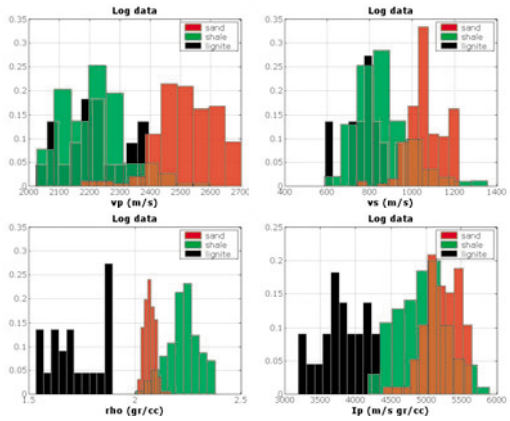


Figure 3: Histograms of P-wave velocity (Vp), S-wave velocity (Vs), density (rho), and acoustic impedance (Ip) for the reference well, color-coded by prior groups.

Assuming that log measurements were a good representation of sand, shale, and lignite properties in the study area, we extended the data doing correlated Monte Carlo (MC) simulation. For each lithology group, 10,000 Vp, Vs, and ρ values where generated. Statistics of logs and MC data were compared, and their similarity was verified. With the extended Vp, Vs, and ρ values, a set of intervallic seismic attributes were calculated for each prior defined lithology group. Then, non-parametric probability density functions (pdf's) of attributes conditioned to the group (sands, shales, and lignites) were estimated. Finally, with the derived pdf's, the Bayesian confusion matrix was estimated to get the conditional probabilities of true group given a predicted group.

Only pairs of intervallic attributes with well-established physical meaning were analyzed: ρλ–ρμ, λ–μ, Ip-EI(30),

Downloaded 09/27/18 to 50.203.133.34. Redistribution subject to SEG license or copyright; see Terms of Use at http://library.seg.org/



PSEI(10)-PSEI(50). λ and μ are Lame's parameters, Ip (=ρVp), is the acoustic impedance, EI(30) is the PP "elastic impedance" for 30°, and PSEI(10) and PSEI(50), are PS "elastic impedances" for incidence angles of 10° and 50° respectively. The first three pairs of attributes can be obtained from PP seismic data, and with them, AVO variations are included in the analysis. Figure 4 gives the diagonal elements of the Bayesian confusion matrix obtained with each of the 4 pairs of attributes. These diagonal elements are the probabilities Prob(true group = X | predicted group = X), with X= sand, shale, or lignite. For a good classification, obviously these diagonal values should be close to 1. It is clear (Figure 4) that PSEI(10)-PSEI(50) is indeed the best attribute combination (amongst those analyzed) to discriminate all 3 groups.

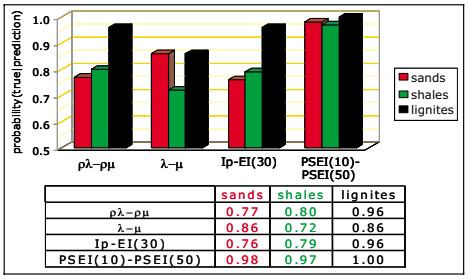


| | sands | shales | lignites |
|---|---|---|---|
| ρλ–ρμ | 0.77 | 0.80 | 0.96 |
| λ–μ | 0.86 | 0.72 | 0.86 |
| Ip-EI(30) | 0.76 | 0.79 | 0.96 |
| PSEI(10)-PSEI(50) | 0.98 | 0.97 | 1.00 |

Figure 4: Conditional probability of the true lithology group given the prediction (diagonal elements of the Bayesian confusion matrix) for the 4 pairs of attributes studied.

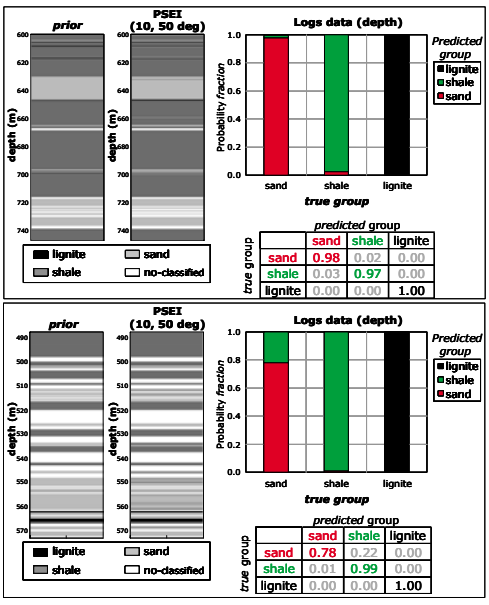


Figure 5: Reference well (top) and Well-2 (bottom). Left: manual classification of each depth level based on gr and ρ thresholds (prior), and ob Bayesian classification using PSEI(10) and PSEI(50) logs. Right: corresponding Bayesian confusion matrix.

Once the class conditioned probabilities, P(attributes | group) are estimated, Bayes rule was used to get P(group | attributes) which is then used to classify the data and predict the probabilities for each group given the attributes. In Figure 5, manual classification of each depth level using cutoff values of gr and ρ logs (prior), is compared to the Bayesian classification using PSEI(10) and PSEI(50). The comparison is done for the reference well and for a second validation well (well 2) located 40 km apart. The pdf's used to classify both wells were calculated using only the training data from the reference well logs. As can be seen, for each well, good classification results were obtained. To get a quantitative estimate of this, Bayesian confusion matrix was calculated, taking the "prior" manually classified groups as the true.

The classification is almost perfect in reference well case. For "well 2", shales and lignites are completely discriminated, but there is 22% probability to erroneously predict shales when they are actually sands. But this uncertainty is still smaller than any obtained using other attributes in the best cases condition when classifying with pdf's defined in the same well.

**Partial Gas Saturation: Fizz Water & Commercial Gas Eastern Venezuela example**

To test the possibility of discriminating between fizz water and commercial gas saturations with PSEI, we used logs data from an Eastern Venezuela well. The sandstones are not well consolidated, and are deposited in shallow to shelf marine environments during the Tertiary. Although in these sandstones commercial gas and fizz water have been found (showing similar PP attributes signatures), the available logs only sample fully water saturated zones. Gassmann's equations were used to substitute in-place water by homogeneous mixtures of gas and water covering a range of gas saturations. Elastic properties of each fluid component at reservoir conditions were calculated using Batzle and Wang (1992) equations. Effective fluid modulus and density were calculated with Reuss and arithmetic average respectively, for water saturations of 0.7, 0.5, 0.3, and 0 (Sw = 1-Sg).

Original logs and resulting logs after fluid substitution are displayed in Figure 6. Notice the abrupt jump in Vp with the initial presence of a small amount of gas. In contrast the density varies more gradually and linearly with gas saturation. Vs does not vary much with gas saturation. As noted by Berryman et al. (2002) the linear behavior of density with saturation makes attributes that are closely related to density useful proxies for estimating gas saturation.

Downloaded 09/27/18 to 50.203.133.34. Redistribution subject to SEG license or copyright; see Terms of Use at http://library.seg.org/

# Far offset P-to-S "elastic impedance" for lithology and partial gas saturation (fizz water) identification

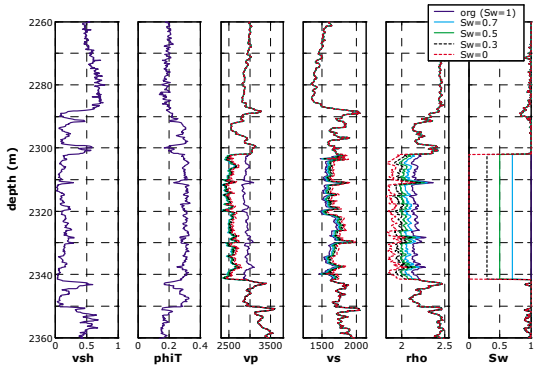


Figure 6: Logs of the available well located in Eastern Venezuela (blue lines), and the resulting logs after fluid substitution (Gassmann) with different water (Sw) and gas (1-Sw) saturations.

PSEI values for incidence angles of 10° and 50° were calculated with original (Sw=1) and Gassmann simulated logs. Additionally, we extended the data points applying MC correlated simulation, and calculated the corresponding pdf's for all modeled Sw situations (Figure 7). In PSEI(10)-PSEI(50) plane, shales are well separated from sands for any Sw. Hence, PSEI for lithology identification is also feasible in this area. However, the important result that we want to emphasize here is the real possibility of discriminating between different homogeneous water (or gas) saturations. Values of PSEI at 10° and 50° *monotonically* decrease with reduction of gas concentration.

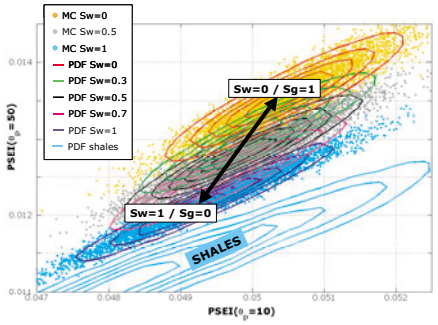


Figure 7: PSEI for incidence angles of 10 and 50 degrees MC simulated values for Sw=0, 0.5, 1, and estimated pdf's for shales, and sands with Sw=0, 0.3, 0.5, 0.7, and 1.

To compare the seismic attributes' ability to discriminate between different gas concentrations, the same procedure as explained for the Orinoco Belt example was followed. Two groups were a-priori defined: "fizz water" ($0.1 < Sg < 0.2$), and "gas" ($Sg > 0.5$). Figure 8 shows the diagonal elements of the Bayesian confusion matrix for each pair of attributes analyzed. It reveals that in this case PSEI(10)-PSEI(50) is the best choice (among those compared) for distinguishing "fizz water" from "commercial gas".

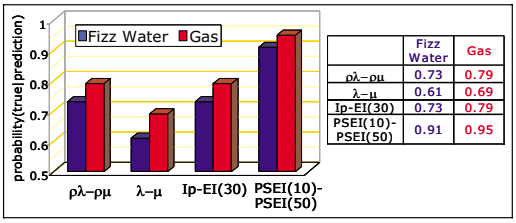


| | Fizz Water | Gas |
|---|---|---|
| ρλ–ρμ | 0.73 | 0.79 |
| λ–μ | 0.61 | 0.69 |
| Ip-EI(30) | 0.73 | 0.79 |
| PSEI(10)-PSEI(50) | 0.91 | 0.95 |

Figure 8: Conditional probability of the true group ("fizz water", commercial gas") given the prediction (diagonal elements of the Bayesian confusion matrix) for the 4 pairs of attributes studied.

## Conclusions

A formulation of P-to-S "elastic impedance" (PSEI), assuming the validity of convolutional model for PS converted waves and weak contrast between layers was presented. The value of incidence angle at which PSEI gives a direct estimation of density was derived. In practice, though it will be difficult to *estimate* absolute densities from PSEI, it will be possible to *classify* reservoir conditions based on relative density variations. An advantage of using two PSEI attributes, instead combination of PP-PSEI is that the PP and PS data time matching is avoided. For Orinoco Belt well logs analyzed, we obtained that PSEI is the best attribute to discriminate lithology (compared with: ρλ–ρμ, λ–μ, Ip-EI(30)). This result can be extended to reservoirs with small acoustic impedance contrast. Finally, using Eastern Venezuela well logs, we showed that increments of Sg (homogenous gas-water mix) monotonically increase PSEI values. Consequently, it is possible to discriminate between fizz water and commercial gas concentration using PSEI.

## References

Batzle, M. and Wang, Z., 1992, Seismic properties of pore fluids; Geophysics, 57, 1396-1408.

Berryman, J. G., Berge, P. A., Bonner, B. P., 2002, Estimating rock porosity and fluid saturation using only seismic velocities; Geophysics, 67, 391-404.

Connolly, P., 1999, Elastic impedance; The Leading Edge, 18, N. 4, 438-452

Engelmark, F., 2000, Using converted shear waves to image reservoirs with low-impedance contrast; TLE, 19, N. 6, 600-603.

Landro, M., Duffaut, K. and Rogno, H., 1999, Well calibration of seabed seismic data; 69th Ann. Internat. Mtg: Soc. of Expl. Geophys., 860-863.

Mukerji, T., Avseth, P., Mavko, G, Takahashi, I., and Gonzalez, E. F., 2001, Statistical rock physics: Combining rock physics, information theory, and geostatistics to reduce uncertainty in seismic reservoir characterization; TLE, 20, N. 3, 313-319.

Wu, Y., 2000, Estimation of gas saturation using P-to-S converted waves; 70th Ann. Internat. Mtg: Soc. of Expl. Geophys., 158-161.

Zhu, F., Gibson, R. L., Atkins, J., and Yuh, S. H., 2000, Distinguishing fizz gas from commercial gas reservoirs using multicomponent seismic data; TLE, 19, N. 11, 1238-1245.